Vehicle System Dynamics
Vol. 00, No. 00, January 2008, 1–16

Original research

Car driving at the limit by adaptive linear optimal preview control

M. Thommyppillai†* , S. Evangelou† and R. S. Sharp‡

†*Departments of Electrical and Electronic Engineering and Mechanical Engineering, Imperial College, London SW7 2AZ, UK*; ‡*School of Engineering, University of Surrey, Guildford, GU2 7XH, UK*

(*v2*)

The paper is concerned with modelling car drivers. The context of the work presented is explained. Then, previous research on the application of optimal linear preview control theory to driving road vehicles with only modest excursions from a straight-running equilibrium state is extended into the general large-lateral-motion arena. Optimal controls are found for steady-cornering trim states of an exemplary car at a given speed as a function of cornering effort, up to the practical limit. The manner in which the optimal controls change as the cornering vigour changes is discussed. Simulations of the virtual driver-controlled car are shown to demonstrate the closed-loop system following lateral path demands and the advantages of employing gain-scheduled adaptive control over a fixed control scheme are demonstrated.

Keywords: Car, driver, preview, optimal, adaptive, simulation

Nomenclature

a, b	car dimensions, figure 1
g	acceleration due to gravity
k	discrete-time counter
n	number of preview points
$\boldsymbol{q}$	diagonal weighting matrix
r	car yaw rate
u	car forward speed
v	car lateral speed
x, y	displacements of car reference point from origin
$\boldsymbol{z}$	full system state vector
$\boldsymbol{A}$, $\boldsymbol{B}$, $\boldsymbol{C}$, $\boldsymbol{E}$	state-space matrices
B_m, C_m, D_m, E_m	Magic Formula tyre lateral force parameters
F_x, F_y	tyre shear forces, figure 1
G	steering gear ratio
I_z	car yaw inertia
J	cost function
$\boldsymbol{K}$	optimal control gain vector
M	car mass
$\boldsymbol{P}$	Riccati matrix
$\boldsymbol{Q}$	weighting matrix

*Corresponding author. Email: mark.thommyppillai@imperial.ac.uk

ISSN: 0042-3114 print/ISSN 1744-5159 online

DOI: 10.1080/0042311YYxxxxxxxx
http://www.informaworld.com

R	control weighting constant
T	discrete time step
α	lateral slip ratio
δ_{sw}	steering wheel angle
η	road lateral displacement from x-axis reference
τ	control input
τ^*	optimal control
subscripts	f, front; l, left; r, rear or right or road; v, vehicle; 1, feedback; 2, preview; dem, demand

1. Introduction

The work described is about modelling car drivers. Such work can be motivated by requirements to:

(i) understand driving and the interactions between car and driver;
(ii) simulate car manoeuvres that are defined by trajectory rather than control input;
(iii) evaluate and improve car handling qualities;
(iv) understand system performance degradation through tiredness, alcohol consumption etc.;
(v) reconstruct accident events;
(vi) use a driver model to explore the full capabilities of a car in a virtual world.

These various motivations are discussed in substantial reviews of driver modelling, see [1–3].

Here the objective is in category (vi) above, connected with the rapid computation of the fastest lap possible for a defined race-car on a defined circuit. In previous research, the fastest lap problem has been treated as simply involving optimization, [4–14] and, although successful outcomes have been achieved, particularly by Gerdts et al in their recent work, the necessary computations have been both complex and lengthy. In that prior work, the path to be followed by the vehicle was part of the optimization problem. However, if the path is given, it appears possible to solve the minimum-time problem by combination of a high-quality tracking controller with a learning process to set speed targets, such that the capacity of the vehicle is fully exploited.

It has become the conventional wisdom that effective driving involves using information from ahead of the vehicle for control purposes [1–3], so-called preview, model-predictive or receding-horizon control [15–19]. At an anecdotal level, one only has to imagine trying to drive in the dark, guided by headlights which illuminate the road only to the side of one's vehicle, to appreciate the loss of facility implied by the lack of any preview information.

Although nonlinear model-predictive control (NMPC) theory has been developed and used extensively [15, 16, 20, 21], general truths about optimal preview control come more readily from linear theory [22–32]. Among these truths are that:

(i) beyond a problem-dependent extent, the returns available from increasing the preview available diminish towards zero. Thus finite-horizon control will approximate infinite-horizon control to arbitrary accuracy;
(ii) tight and loose controls can be designed by varying the relative weightings of tracking accuracy and control power. Optimal linear preview control is not just one scheme but is one of a whole family of schemes, for a given problem;
(iii) tight control requires relatively short previews and yields relatively large

control efforts and conversely;

(iv) optimal linear quadratic preview controls for time-invariant systems are of state-feedback form and can be found off-line. The state which is fed back is that of the plant augmented with a shift register or delay-line, thus involving the preview information;

(v) near-perfect tracking occurs with optimal linear systems within a frequency range that extends as the control tightness increases. The best that can be achieved depends on the problem, of course.

The development, through the application of linear optimal preview control theory, of high-quality longitudinal controllers is documented in [29, 32] and of lateral controllers in [26–28, 30, 31]. Longitudinal and lateral problems have recently been combined in [33] but attention here will be focused on the lateral problem only. Our car will be controlled to travel at substantially constant speed by a simple feedback controller. The obvious limitation of linear controls arises from the essential nature of tyre shear forces, the main source of external influence, which limit and then decrease with increasing slip.

The dynamic characteristics of a car vary strongly with speed, especially when the performance limits are extended by aerodynamically generated downforce, increasing the frictional coupling between the tyres and the ground. Within an operating range around the straight-running state, a linear representation of a (good) car can be expected to be accurate. As manoeuvring severity increases, tyre shear forces saturate in a smooth and progressive manner. Optimal controls derived assuming linearity can be expected to work well for gentle manoeuvring and not so well for limit operation therefore. A racing driver can be expected to know the dynamics of his/her car perfectly, since an important part of his/her function is to continually update his/her internal model of the system, based on recent experience. Optimality of controls is vital. Robustness is not so important.

Neglecting practical issues relating to computing time, standard NMPC theory would provide virtual racing driver designs, in numerical form, straightforwardly [34]. Such theory involves discretising the description of the path demands ahead of the vehicle and of the control history within the preview/control horizon. Then, at each computational step, a complex optimization problem has to be solved on-line. Convergence to the global optimum is not guaranteed. From any solution obtained, only the first step is used for control. The process is slow and extravagant. Compromise between accuracy of solution and speed of computation is essential.

Methods for simplifying NMPC calculations include:

(i) shortening the preview and control horizons. Using foreshortened previews may spoil the results, even yielding instability for the controlled system [15, 16]. In the limit, single-point preview and a single control level may be employed but the results are likely to be poor [1];

(ii) linearizing the plant model for control calculation purposes [2, 17–19];

(iii) using a simplified plant model for control design purposes, especially if a system with special and useful features approximating the *real* plant can be found [35, 36].

Many examples of successful (virtual) tracking incorporating such simplifications can be found in the literature but it should be noted that modest tracking capabilities are quite easy to realize, while racing-driver performance levels are very high and will not be achieved readily.

Worthy of note in connection with (ii) above are the approaches of [17] and of [18, 19]. In the former, a simplified car, being nonlinear only in respect of its tyre-force characteristics at front and rear axles, is represented on-line as having

linear tyres appropriate to the region local to the current axle sideslip values. The predicted motion over the optimization horizon is computed as a superposition of the car trajectory from the current state for zero steer input, the complementary function, and the response to the steering input applied over the control horizon, the particular integral. The *driver* starts with a knowledge of tyre cornering stiffnesses for a number of combinations of front and rear axle sideslips. While this approach to nonlinear vehicle control is effective at the simple car model level used, it seems likely that the method will become infeasible if the vehicle model is more general, containing a substantially greater number of nonlinearities.

In the latter case, the nonlinear system is linearized for small variations from the present state at each time step, yielding a family of linear systems, varying with time in a manner that can only be known on-line. The response predicted is obtained by superposition of the locally linearized system's response to variations from the current control input plus the nominal state trajectory, which is that corresponding to the current control input being sustained without change. The current optimization requires that the trajectory of the locally linearized system stay close to that of the nonlinear system of real interest over the optimization horizon, which implies some conflict between the need for a long optimization horizon, to deal with the preview information properly, and the need for the locally linearized car to stay close to the trajectory of the nonlinear car. The tracking quality reported appears to be rather poor, suggesting that the preview is not fully utilised in the computations completed. Several parameters are influential, including the discrete time step, the optimization horizon and the control horizon, and it might be that changes to the parameters would improve the quality.

To obtain the desired balance between speed of computation and vehicle control capability, we employ off-line-computed optimal linear controls, with adaptation to deal with the progressive and smooth saturating nonlinearity of the tyre shear forces. We suppose that the well-controlled behaviour of a car always involves operation close to a trim state. Our theoretical driver pulls from memory a control design that is appropriate to current operating conditions. The various control schemes needed are prepared off-line, through the generation of many trim states by simulation, linearization for small perturbations about each trim state and application of linear optimal preview control software. Optimal control sets are stored and retrieved as required for manoeuvring simulations. With the present restriction to constant-speed running, the family of trim states necessary to cover general running conditions is parametrized by forward speed and front-axle-lateral-slip ratio.

In the next section, the car model is described. The linear optimal preview control theory relied upon is then outlined. After that, we describe the use of open-loop simulation runs to find trim or dynamic equilibrium states for the vehicle. Optimal controls are then discussed. Simulations of the closed-loop lateral path-tracking system are described subsequently, with evaluation of the control adaptation. Finally, conclusions are drawn.

2. Vehicle Model

The car model employed involves longitudinal, lateral and yaw freedoms of a single rigid body, this being a standard in vehicle dynamics [37, 38]. The model needs to be written such that the absolute lateral displacement of the car reference point is an output, since this displacement has to be compared with that of the road, in an inertial reference frame, in setting up the optimal steering control problem, see [26–28, 30, 31]. The car is illustrated in figure 1. Steering wheel rotation controls the notional front road wheel steer angle, δ, through a gear ratio, G.

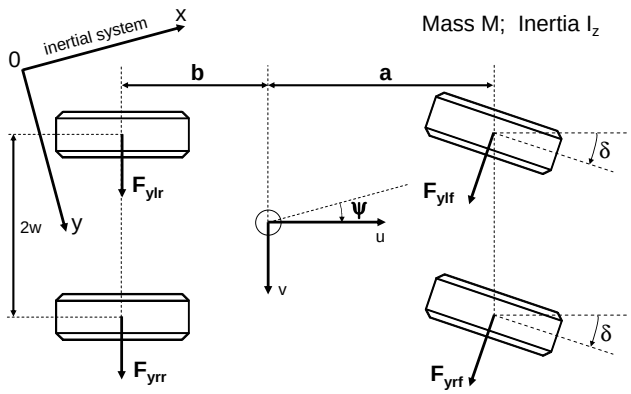

Figure 1. Plan view of simple car confined to plane motion with 3 degrees of freedom.

The kinematic equations for the car are:

$$\dot{x} = u\cos\psi - v\sin\psi$$

$$\dot{y} = v\cos\psi + u\sin\psi$$

$$\dot{\psi} = r$$

while the dynamic equations are:

$$M\left(\dot{u} - vr\right) = F_x - \left(F_{ylf} + F_{yrf}\right)\sin\delta$$

$$M\left(\dot{v} + ur\right) = F_{ylr} + F_{yrr} + \left(F_{ylf} + F_{yrf}\right)\cos\delta$$

$$I_z\dot{r} = b\left(F_{ylr} + F_{yrr}\right) - a\left(F_{ylf} + F_{yrf}\right)\cos\delta$$

The forward speed of the car is maintained at a constant level by the action of a proportional, integral, differential (PID) controller, giving rise to the driving force at the mass centre, F_x, resulting from speed error. The two tyres of each axle are lumped together with respect to shear force development and are taken to generate only lateral forces in response to lateral slip, with *Magic Formula* style [38]. Specifically:

$$F_y = 2D_m\sin\left[C_m\arctan\left(B_m\alpha - E_m\left(B_m\alpha - \arctan\left(B_m\alpha\right)\right)\right)\right]$$

with lateral slip ratio, α, ignoring small differences between left and right sides of the car, given by

$$\alpha_f = \frac{u\sin\delta - \left(v + ar\right)\cos\delta}{u\cos\delta + \left(v + ar\right)\sin\delta}$$

Table 1. Parameters, symbols and values for car and tyres.

Parameter	Symbol	Value
Mass	M	1050 kg
Yaw inertia	I_z	1500 kgm^2
Mass centre to front axle distance	a	0.92 m
Mass centre to rear axle distance	b	1.38 m
Steering gear ratio	G	17
Stiffness factor (per tyre)	B_m	17.5
Shape factor (per tyre)	C_m	1.68
Peak factor (per tyre)	D_m	3900 N
Curvature factor (per tyre)	E_m	0.6

for the front and

$$\alpha_r = \frac{br - v}{u}$$

for the rear, with $\delta = \frac{\delta_{sw}}{G}$, δ_{sw} being the steering wheel angle and G being the steering gear ratio. Parameter values of the car and tyres are given in Table 1 and the tyre lateral force versus slip relationship is shown in figure 2. The lateral force available at each axle is 7800 N, which exceeds the static axle loads of 6180.3 N front and 4120.2 N rear by some margin. The car is therefore capable of front-axle-limited steady-state cornering at $\frac{7800g}{6180.3} = 12.38\, m/s^2$ lateral acceleration.

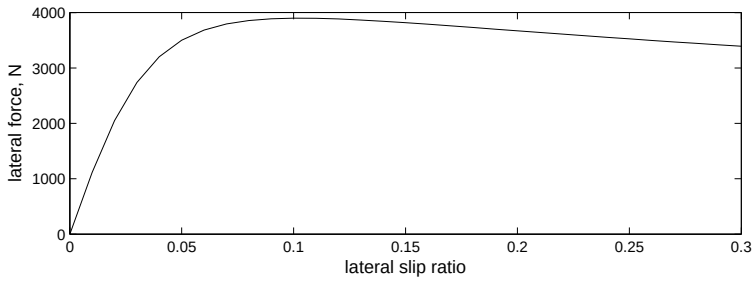

Figure 2. Lateral force as a function of lateral slip ratio for each tyre.

3. Optimal Linear Preview Control Theory

In studies of preview steering control already completed, a linear vehicle model is arranged to include the absolute lateral displacement of its reference point as a state and to have steering torque or steering displacement as a primary control input. The model is put into discrete-time form, using a time step of T say. Through each time step, the vehicle travels uT where u is the specified speed. A roadway lateral profile is defined by discrete points uT apart longitudinally in the inertial reference system, so that all the road profile points in front of the vehicle approach it by uT through each time step. In this inertial reference system, illustrated in figure 3, the road dynamics are those of a shift register or delay line and the equations describing these dynamics are of the same form as the equations of the vehicle. The two sets of equations are combined to yield a compound system, with its state-vector having a partition for the vehicle and a partition for the road. At this first stage, there is no coupling between the parts.

Suppose the vehicle equations are:

$$\boldsymbol{x_v}(k+1) = \boldsymbol{A_v}\boldsymbol{x_v}(k) + \boldsymbol{B_v}\tau(k)$$

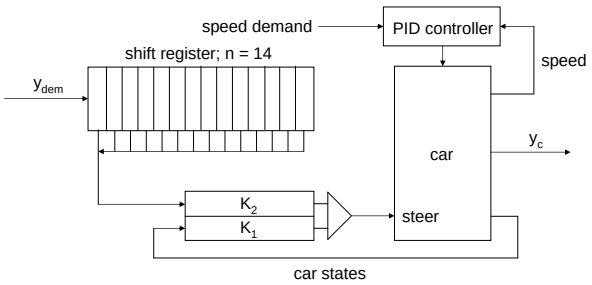

Figure 3. Diagrammatic representation of a car tracking a roadway path at constant speed, with the whole system referenced to ground. Such a description implies that the road sample values pass through a serial-in, parallel-out shift register operation at each time step. y_{dem} is the previewable lateral displacement signal. $\boldsymbol{K_1}$ represents the full car-state feedback control, while $\boldsymbol{K_2}$ represents the preview control, in the form of feedback of the shift register states.

$$\boldsymbol{y_v}(k) = \boldsymbol{C_v}\boldsymbol{x_v}(k)$$

with discrete-time counter k, vehicle state vector $\boldsymbol{x_v}$ and single control input τ, and let the road equation be:

$$\boldsymbol{\eta_r}(k+1) = \boldsymbol{A_r}\boldsymbol{\eta_r}(k) + \boldsymbol{B_r}\eta_{rn}(k)$$

with road state $\boldsymbol{\eta_r}$ and road sample values that enter the system at time kT being η_{rn}, a scalar representing y-displacement demands. For n preview points, $\boldsymbol{\eta_r}$ is (n x 1).

To represent the road shift register process, $\boldsymbol{A_r}$ is (n x n) and has the form:

$$\boldsymbol{A_r} = \begin{bmatrix} 0 & 1 & 0 \dots 0 \\ 0 & 0 & 1 \dots 0 \\ \vdots & \vdots & \vdots \ddots \vdots \\ 0 & 0 & 0 \dots 1 \\ 0 & 0 & 0 \dots 0 \end{bmatrix}$$

and $\boldsymbol{B_r}$ is (n x 1), corresponding to the single previewable disturbance, and has the form:

$$\boldsymbol{B_r} = \begin{bmatrix} 0\,0\,0\,0\,0\,0 \dots 0\,1 \end{bmatrix}^{\boldsymbol{T}}$$

Combining vehicle and road equations together, the full dynamic system is defined by:

$$\begin{bmatrix} \boldsymbol{x_v}(k+1) \\ \boldsymbol{\eta_r}(k+1) \end{bmatrix} = \begin{bmatrix} \boldsymbol{A_v} & 0 \\ 0 & \boldsymbol{A_r} \end{bmatrix} \begin{bmatrix} \boldsymbol{x_v}(k) \\ \boldsymbol{\eta_r}(k) \end{bmatrix} + \begin{bmatrix} \boldsymbol{B_v} \\ 0 \end{bmatrix} \tau(k) + \begin{bmatrix} 0 \\ \boldsymbol{B_r} \end{bmatrix} \eta_{rn}(k)$$

which takes the standard discrete-time form:

$$\boldsymbol{z}(k+1) = \boldsymbol{A}\boldsymbol{z}(k) + \boldsymbol{B}\tau(k) + \boldsymbol{E}\eta_{rn}(k)$$

$$\boldsymbol{y}(k) = \boldsymbol{C}\boldsymbol{z}(k)$$

If η_{rn} is a sample from a white-noise random sequence, the time-invariant optimal control which minimizes a quadratic cost function J, given that the pair $(\boldsymbol{A}, \boldsymbol{B})$ is

stabilizable and that the pair $(\boldsymbol{A}, \boldsymbol{C})$ is detectable [39], is:

$$\tau^*(k) = -\boldsymbol{K}\boldsymbol{z}(k)$$

where $\boldsymbol{K} = \left(R + \boldsymbol{B}^{\boldsymbol{T}}\boldsymbol{P}\boldsymbol{B}\right)^{-1}\boldsymbol{B}^{\boldsymbol{T}}\boldsymbol{P}\boldsymbol{A}$, given that the cost function J is:

$$J = \lim_{n\to\infty}\sum_{k=0}^{n}\{\boldsymbol{z}^{\boldsymbol{T}}(k)\boldsymbol{Q}\boldsymbol{z}(k) + \tau^2(k)R\}$$

and $\boldsymbol{P}$ satisfies the matrix-difference-Riccati equation:

$$\boldsymbol{P} = \boldsymbol{A}^{\boldsymbol{T}}\boldsymbol{P}\boldsymbol{A} - \boldsymbol{A}^{\boldsymbol{T}}\boldsymbol{P}\boldsymbol{B}\left(R + \boldsymbol{B}^{\boldsymbol{T}}\boldsymbol{P}\boldsymbol{B}\right)^{-1}\boldsymbol{B}^{\boldsymbol{T}}\boldsymbol{P}\boldsymbol{A} + \boldsymbol{Q}$$

Here $\boldsymbol{Q} = \boldsymbol{C}^{\boldsymbol{T}}\boldsymbol{q}\boldsymbol{C}$ and $\boldsymbol{q}$ is a diagonal weighting matrix, diag[q_1, q_2, ...], with terms corresponding to the number of performance aspects contributing to the cost function, and R is a scalar weighting on the control input, the steering wheel angle. $\boldsymbol{C}$ is chosen such that the quadratic term $\boldsymbol{z}^{\boldsymbol{T}}(k)\boldsymbol{Q}\boldsymbol{z}(k)$ in the cost function J penalizes the sum of the squares of the differences between the y-coordinate of the car's reference point and the corresponding absolute lateral displacement of the road, over the optimization horizon.

The optimal controls are found by first solving the standard non-preview linear quadratic regulator problem to yield the car-state-feedback control and then using a recursive computation to give each preview gain in sequence, applying to points further out from the car as the sequence progresses. The method is described in more detail in [25, 26, 29, 31, 40]. A recently available alternative for finding optimal preview controls is provided by a toolbox for MATLAB [41], see also http://code.google.com/p/preview-control-toolbox/. The preview gains $\boldsymbol{K_2}$, see figure 3, inevitably fall to zero as the preview distance increases, so that the number of preview points included can be chosen, by trials, so that effectively the full benefit available is obtained. This is referred to as *full* preview. Only full preview control is of interest in the present context.

4. Trim States

Dynamic equilibrium or trim states are generated by simulations designed to take the vehicle through manoeuvres, in each of which the state changes so slowly that any snapshot of the conditions can be taken to represent equilibrium. Variations over a full range of speeds and steer angles need to be covered. Simulation runs involve choosing the speed, relying on the PID speed-error-feedback controller of the driving force to maintain the desired condition, see figure 3, and slowly ramping up the front-axle-lateral-slip-ratio demand over the full range of interest. A slip-error proportional steering controller is incorporated into the model at this stage, so that the steering input is controlled to give the slip demanded. Trim states are stored, after quality checking, for increments of 0.002 in the front-axle-lateral-slip scheduling parameter. Then, a family of linear models, each representing the neighbourhood of a particular trim state is established numerically. Optimal preview controls are subsequently found for each trim.

5. Optimal Controls

Examples of optimal controls are shown in this section. Frequency responses of selected optimally-controlled systems are also depicted. Each set of controls generated requires the setting of:

(i) the discrete time step, here always 0.01 s;
(ii) the trim state from which small perturbations are considered to occur. Each trim state is defined by a car speed and a front-axle-lateral-slip ratio. Initially, the lateral acceleration was thought of as the second scheduling parameter, but for high values of the lateral acceleration, there are two trim states corresponding to one value of the acceleration. The front-axle-slip ratio is better in this respect;
(iii) y-tracking error weighting relative to the fixed weighting on control power. All the results shown are for a weighting of 100 on the tracking error, that is q_1=100, and no other performance-cost element. Tighter and looser controls can be engaged by increasing or decreasing respectively this weighting. The closed-loop system bandwidth is higher for tighter control and conversely [27, 32];
(iv) the number of preview points to be used.

Corresponding to each trim state, there is a linearization and, with defined weightings, a set of optimal control gains. $\boldsymbol{K_1}$ is the vector of car-state-feedback gains, while $\boldsymbol{K_2}$ is the vector of shift-register-state-feedback or preview gains. Such preview gain sequences, for a speed of 30 m/s, are shown in figure 4 as functions of front-axle-lateral-slip ratio. A selection of car-state-feedback gains relating to lateral velocity and yaw velocity for the same speed is shown in Table 2 and, for clarity, the two-dimensional slices of figure 4 belonging to the same front-axle-slip ratios as for Table 2, are shown in figure 5.

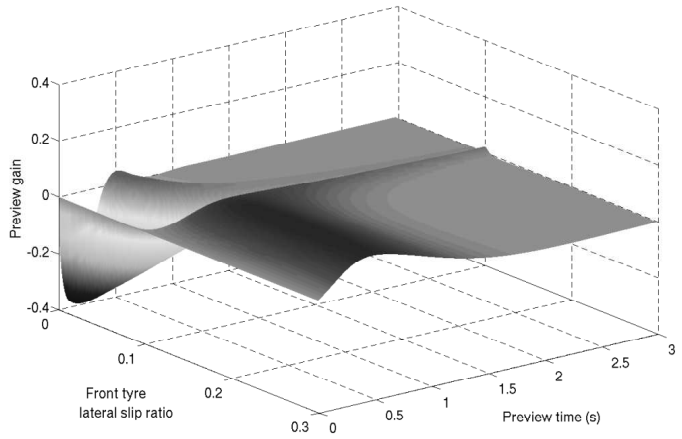

Figure 4. Three-dimensional plot of $\boldsymbol{K_2}$ preview gain sequences as functions of front-axle-lateral-slip ratio, representing the cornering-effort level.

As the cornering effort increases, the control authority decreases and the influence on the preview control is to reduce the gains and to lengthen the preview needed for full performance. When the front-axle-slip ratio exceeds that for maximum force, see figure 2, the relationship between slip ratio change and force change is the reverse of the normal one. Correspondingly, the preview gains change sign. On

Table 2. Car-state-feedback gains relating to lateral and yaw velocities for a car speed of 30 m/s and four different trim states defined by front-axle-slip ratio.

Slip ratio	0	0.04	0.06	0.40
Lateral velocity	0.5971	1.3639	2.4931	-5.7844
Yaw velocity	0.9767	1.9513	3.1738	-5.7633

the contrary, the reducing control authority causes the optimal feedback gains to increase but the sign reversal occurs here also, see Table 2.

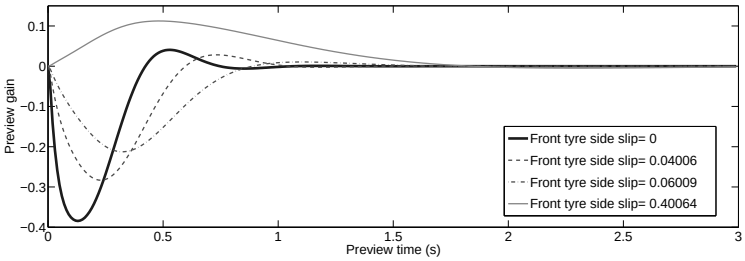

Figure 5. Two dimensional plot of $\boldsymbol{K_2}$ preview gains, for car speed of 30 m/s and trim states defined by four different front-axle-slip ratios.

Frequency responses of the closed-loop, driver-controlled car at 30 m/s speed are shown in Bode form in figure 6, for four levels of cornering effort defined by the front-axle-lateral-slip ratio. Deriving from the decreasing control authority as the car corners more vigorously and uses up tyre friction forces in the trim condition, the system bandwidth decreases progressively. The results illustrate how a real driver needs to drive a little short of the absolute limit in the interests of retaining some control capability, the best drivers requiring to leave only the smallest margins.

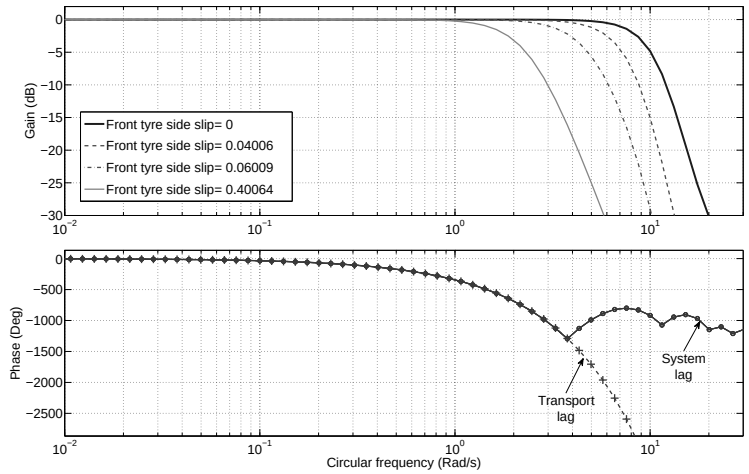

Figure 6. Frequency responses in Bode plot form for driver-controlled car at 30 m/s speed and trim states defined by four different front-axle-slip ratios.

6. Tracking Simulation Results

To demonstrate the application of the optimal preview controls, tracking a lateral position target sequence at a challenging speed by the driver-controlled car is sim-

ulated on a variety of paths. The same manoeuvre with both non-adaptive-driver control corresponding to the straight-running trim state only, and with adaptive-gain-scheduled control, corresponding to the range of trim states depicted in figure 4, are shown and contrasted. At the commencement of each manoeuvre, the reference trim state involves straight running, which remains the case when non-adaptive control is employed. When the control is adaptive, the reference trim state changes, implying not only discrete gain changes but also changes in the way in which the preview path errors are measured. The situations are depicted in figure 7.

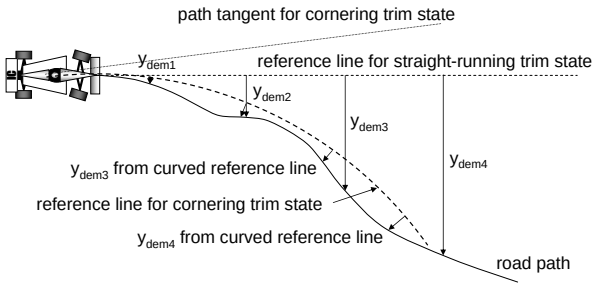

Figure 7. Illustration of the implications of adapting the controls to the trim state. The basis for measuring the previewed path errors becomes a circular arc when the reference state involves turning. Also, the steering wheel angles derived from the controller are increments that have to be added to the appropriate trim-state value to get the actual steer angle.

To further illustrate the gain-scheduling process, suppose that schedule "i" is in place and that, at the end of the next simulation step, the front-axle-slip ratio indicates schedule "i+1" to be the nearest to the new running state. The current car states and input must be expressed as increments from the "i+1" trim states, the feedback control operating on these increments, using the "i+1" trim-state $\boldsymbol{K_1}$ values. The preview errors are obtained by transforming the road data in front of the car into a driver's view frame of reference and sampling the road ahead relative to the driver's curved optical lever, see figure 7, with the curvature being that belonging to the trim state "i+1". The preview errors are operated on by the "i+1" trim-state gains, $\boldsymbol{K_2}$, to give the feedforward contribution to the steering input.

Under some circumstances, the switching from one reference system to another neighbouring one can contribute to the vehicle and controls becoming oscillatorily unstable. The *driver* has infinite bandwidth, so that all the changes are instantaneous at a switching point, and this is an important part of the problem. The instability can be prevented by including rate limiting on the steering wheel motion, a reasonable limit from the real world of car driving being 9 rad/s [42]. This limit is sufficiently high to not interfere with the steering control required to follow the path but it is also stabilizing. Further, it is non-critical, since the tracking results are similar for rate limits down to 3 rad/s. A steering wheel rate limit of 9 rad/s is included in the simulation studies to be shown, irrespective of the employment of gain switching.

The controlled cars were asked to track three challenging paths: a *hair-pin* bend, a lane-change and a double *s-bend*, see figure 8. The paths were designed to show the capability of the adaptive controls to achieve good tracking, while the fixed-gain system loses control.

The *hair-pin* starts with a straight section, 72.6m long. This is followed by a change in curvature which is uniform with distance, a clothoid curve, to a radius of 72.6 m. The curvature is then constant over an arc of 0.75π rad. and subsequently

reduces uniformly, another clothoid, until it reaches zero, when a straight section follows.

The lane change begins and ends with a straight section, each 300 m in length and parallel to one another. The finishing straight has a lateral offset of 5 m and a longitudinal offset of 10 m relative to the end of the starting straight. A sinusoidal spline is used to bridge the gap between these two sections.

The double *s-bend* starts with a straight section 330 m in length. This is followed by a right-handed semi-circular section with a radius of 80 m. After a short straight, 30 m in length, a left-handed semi-circular section follows, also with a radius of 80 m. Another short straight, 30 m long, completes the first *s-bend*. The second *s-bend* is similar to the first but has circular arcs with a tighter radius of 75 m. The last circular arc is formed over an angle of 0.9π rad. A straight section tangential to the end of the last arc completes the track.

The speed demanded, 30 m/s, is such that perfect tracking of each path would require slightly more side-force from the front axle than is available, so that control at the absolute limit is exercised.

Tracking errors connected with fixed-gain and gain-scheduled controls when tracking the *hair-pin*, lane-change and double *s-bend* are plotted in figures 9, 11 and 13 respectively. Corresponding time histories for front-axle side-slip and steering wheel angle are shown in figures 10, 12 and 14.

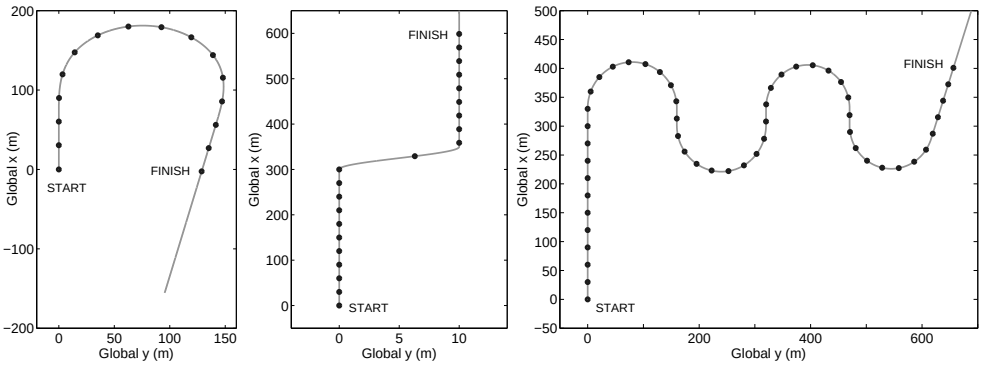

Figure 8. Path demand for 3 manoeuvre simulations showing points at 1 s intervals along them. (a) A *hair-pin*. (b) A lane-change. (c) A double *s-bend*.

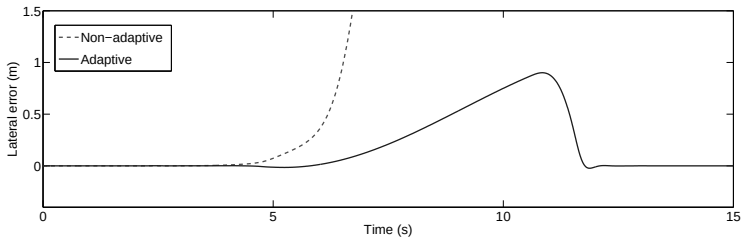

Figure 9. Lateral tracking errors in simulated *hair-pin* manoeuvre at 30 m/s speed with non-adaptive (fixed-gain) or adaptive (gain-scheduled) controls.

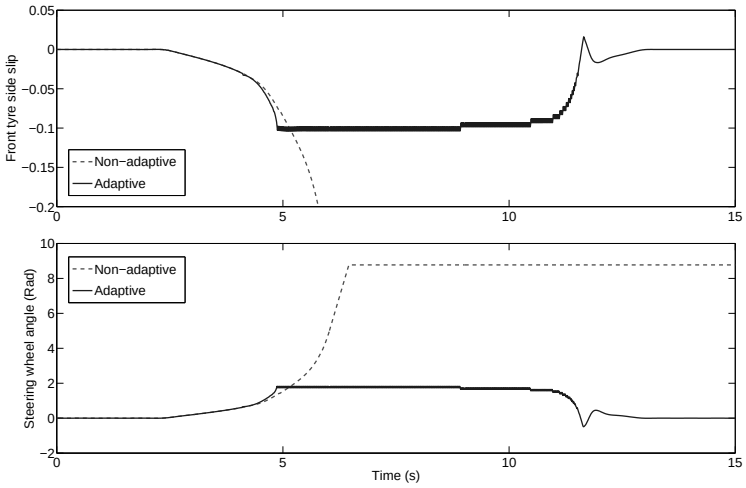

Figure 10. Front-axle side-slip and steering wheel angle histories for *hair-pin* manoeuvre of figure 8 with non-adaptive (fixed-gain) or adaptive (gain-scheduled) controls.

In the *hair-pin* tracking simulation, the front-axle side-force reaches its peak at about 5 s into the run as seen in figure 10. The non-adaptive controller fails to appreciate what is needed to maintain good tracking and the car starts to go out of control. The adaptive controller, on the other hand, adjusts the steering angle such that the front-axle side-force continues at the peak of its capability. The car is going too fast for it to be possible to track the desired course precisely but it does the best that it can. As soon as it becomes possible for the car to align with the path again, it does so. The fixed-gain driver ends using full lock, set at 9 rad in the simulation model, in an attempt to get more side-force, while the adaptive driver uses much more modest control inputs.

A similar situation is observed during the tracking of the lane-change manoeuvre. When the car arrives at the start of the lane-change, about 9.5 s into the simulation, the non-adaptive controller initially follows the same steering demand as the adaptive controller. However, as the lateral error grows, the non-adaptive controller continues to demand a larger steering angle in an attempt to rectify the tracking error. This saturates the front-axle side-force which exacerbates the problem. The steering lock limit is eventually reached and the car loses control as seen in figure 12. The adaptive controller, having knowledge of the full non-linear dynamics of the car, uses a more measured driving style. As a result, the car negotiates the lane change whilst maintaining control and keeping lateral deviation to a minimum.

On the double *s-bend*, the non-adaptive controller is able to negotiate the first *s-bend* without loss of control. However, the tracking error in the period between 11 and 27 s in figure 13 shows the poorer tracking performance of the non-adaptive controller when compared to its adaptive counterpart. The non-adaptive controller fails on entry to the second *s-bend* where, as in previous simulations, it demands more from the front axle when it is already close to saturation. As a result, the non-adaptive controller loses control soon after 30 s. The adaptive controller, however, keeps the front axle very close to its peak side-force capacity and maintains control. After negotiating the tighter second *s-bend*, the controller restores the car to the intended path.

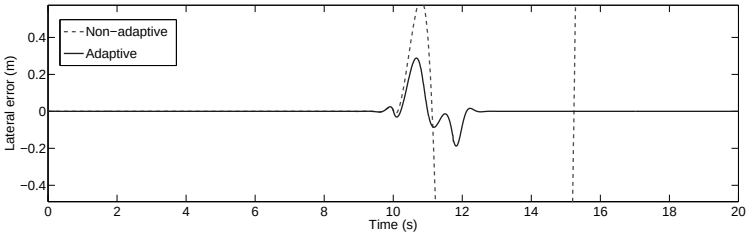

Figure 11. Lateral tracking errors in simulated lane-change manoeuvre at 30 m/s speed with non-adaptive (fixed-gain) or adaptive (gain-scheduled) controls.

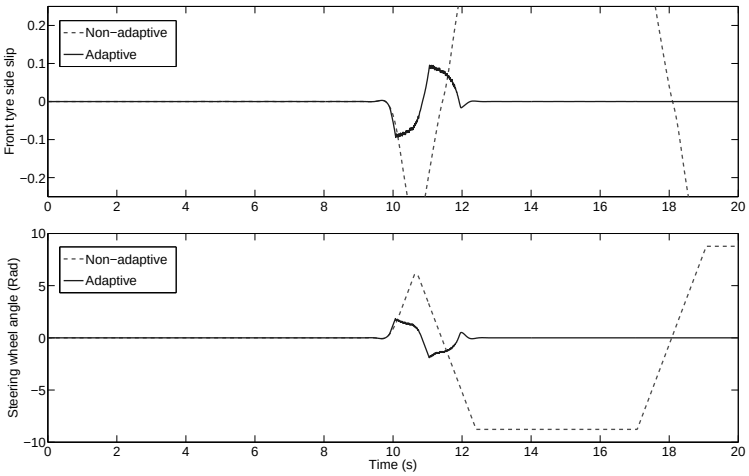

Figure 12. Front-axle side-slip and steering wheel angle histories for lane-change manoeuvre of figure 8 with non-adaptive (fixed-gain) or adaptive (gain-scheduled) controls.

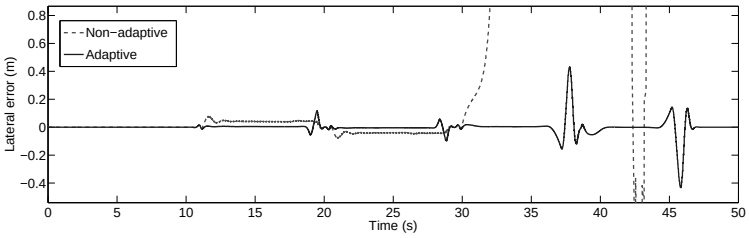

Figure 13. Lateral tracking errors in simulated double *s-bend* manoeuvre at 30 m/s speed with non-adaptive (fixed-gain) or adaptive (gain-scheduled) controls.

7. Conclusion

The work described is motivated by a desire to construct a perfect virtual racing driver, which will be capable of exploiting the full capacity of a racing car. The strategy used depends on the adaptive employment of linear-optimal-preview controls. Prior research has shown how such controls can be found and applied, when only small perturbations from a trim state are involved and the linear control design is based on the relevant trim state. Here, the previous work is extended by the generation of optimal control sets for a full range of cornering effort, as a way of accommodating the saturating nonlinearity of the tyre lateral forces. Optimal control sets vary in a systematic and interesting manner as the tyres work harder. The variations and their interpretation have been discussed. The path-tracking frequency response properties of selected driver-controlled cars have been calculated and discussed also.

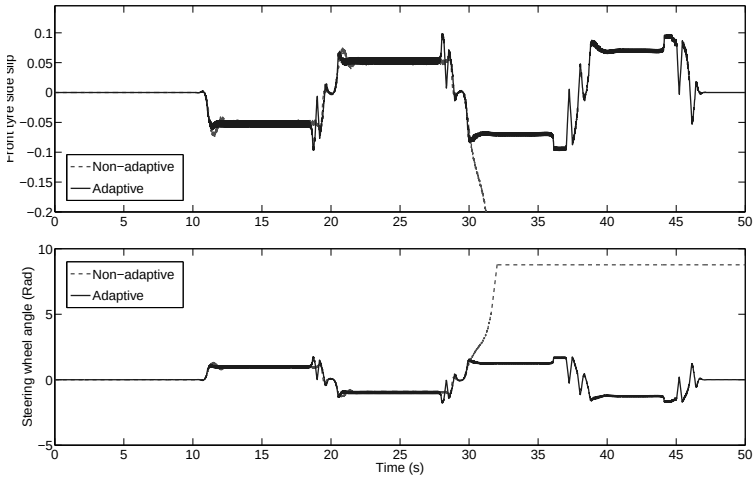

Figure 14. Front-axle side-slip and steering wheel angle histories for double *s-bend* manoeuvre of figure 8 with non-adaptive (fixed-gain) or adaptive (gain-scheduled) controls.

Tracking of three challenging paths at a fixed, high speed by a car and driver with controls based on straight-running only and with an adaptive, gain-scheduling driver have been simulated, with parametrization of the running condition of the car by front-axle-lateral-slip level. Controls for trim states which are very close together have been utilised. To maintain system stability, rate limiting on the steering wheel motion has been found necessary. With rate limiting sufficient for stability but not interfering with required control inputs, gain-switching noise observable in the results is very small. An obvious alternative to discrete gain changing is to use interpolation, which would allow a coarser grid of stored gains to be employed. Excellent path tracking of the adaptive system has been demonstrated, under circumstances for which the fixed-gain controls are inadequate.

Remaining tasks include application of the adaptive controls to variable speed conditions, including limit braking and accelerating, application of the methods to more elaborate vehicles and the inclusion of learning control, so that the driver's speed ambition can be properly related to the tyre-force utilisation observed.

Acknowledgment

The authors are pleased to acknowledge financial support from the UK Engineering and Physical Sciences Research Council and Williams F1.

References

[1] K. Guo and H. Guan, *Modelling of driver/vehicle directional control system*, Vehicle System Dynamics 22(3-4) (1993), pp. 141–184.

[2] C.C. MacAdam, *Understanding and modelling the human driver*, Vehicle System Dynamics 40(1-3) (2003), pp. 101–134.

[3] M. Plöchl and J. Edelmann, *Driver models in automobile dynamics application*, Vehicle System Dynamics 45(7-8) (2007), pp. 699–741.

[4] T. Fujioka and T. Kimura, *Numerical simulation of minimum time cornering behaviour*, JSAE Review 13(1) (1992), pp. 44–51.

[5] J.P.M. Hendrikx, T.J.J. Meijlink, and R.F.C. Kriens, *Application of optimal control theory to inverse simulation of car handling*, Vehicle System Dynamics 26(6) (1996), pp. 449–462.

[6] V. Cossalter et al., *Evaluation of motorcycle manoeuvrability with the optimal manoeuvre method*, SAE 983022 (1998).

[7] V. Cossalter et al., *A general method for the evaluation of vehicle manoeuvrability with special emphasis on motorcycles*, Vehicle System Dynamics 31(2) (1999), pp. 113–135.

[8] D. Casanova, R.S. Sharp, and P. Symonds, *On minimum time optimisation of formula one cars: The influence of vehicle mass*, in *Proc. of the 5th International Symposium on Automotive Control (AVEC 2000)*, August 22–24, , Ann Arbor MI, 2000, pp. 585–592.

[9] D. Casanova, R.S. Sharp, and P. Symonds, *Minimum time manoeuvring: The significance of yaw inertia*, Vehicle System Dynamics 34(2) (2000), pp. 77–115.
[10] D. Casanova et al., *Application of automatic differentiation to race car performance optimisation*, in *Proc. of Automatic Differentiation 2000: From Simulation to Optimization* Springer-Verlag, New York, 2000, pp. 113–121.
[11] D. Casanova, R.S. Sharp, and P. Symonds, *Sensitivity to mass variations of the fastest possible lap of a Formula One car*, Vehicle System Dynamics 35(2) (2001), pp. 119–134.
[12] D. Casanova, R.S. Sharp, and P. Symonds, *On the optimisation of the longitudinal location of the mass centre of a Formula One Car for two circuits*, in *Proc. of the 6^{th} International Symposium on Automotive Control (AVEC 2002)*, September 9–13, , Hiroshima, 2002.
[13] M. Gerdts, *A moving horizon technique for the simulation of automobile test-drives*, Z. Angew. Math. Mech. 83(3) (2003), pp. 147–162.
[14] M. Gerdts et al., *Generating optimal trajectories for an automatically driven car*, Optimization and Engineering (2008). (see http://www.springerlink.com/content/h7264683764xx5rm/)
[15] R. Findeisen and F. Allgöwer, *An introduction to nonlinear model predictive control*, C.W. Scherer and J.M. Schumacher, eds., Dutch Institute of Systems and Control, 2001, pp. 3.1–3.45.
[16] R. Findeisen et al., *State and output feedback nonlinear model predictive control: An overview*, European Journal of Control 9(2-3) (2003), pp. 179–195.
[17] S.D. Keen and D.J. Cole, *Steering control using model predictive control and multiple internal models*, in *Proc. of the 8^{th} International Symposium on Automotive Control (AVEC 2006)*, August 20–24, , Taipei, Taiwan, 2006, pp. 599–604.
[18] P. Falcone et al., *Predictive active steering control for autonomous vehicle systems*, IEEE Trans. Control Syst. Technol. 15(3) (2007), pp. 566–580.
[19] P. Falcone et al., *Linear time-varying model predictive control and its application to active steering systems: Stability analysis and experimental validation*, Int. J. Robust Nonlinear Control 18 (2008), pp. 862–875.
[20] J.B. Rawlings, *Tutorial overview of model predictive control*, IEEE Control Syst. Mag. (2000), pp. 38–52.
[21] S.J. Qin and T.A. Badgwell, *A survey of industrial model predictive control technology*, Control Engineering Practice 11(7) (2003), pp. 733–764.
[22] M. Tomizuka and D.E. Whitney, *Optimal discrete finite preview problems (why and how is future information important?)*, Transactions of ASME, Journal of Dynamic Systems, Measurement, and Control 97(4) (1975), pp. 319–325.
[23] M. Tomizuka, *Optimal linear preview control with application to vehicle suspension - revisited*, Transactions of ASME, Journal of Dynamic Systems, Measurement, and Control 98(3) (1976), pp. 309–315.
[24] N. Louam, D.A. Wilson, and R.S. Sharp, *Optimal control of a vehicle suspension incorporating the time delay between front and rear wheel inputs*, Vehicle System Dynamics 17(6) (1988), pp. 317–336.
[25] G. Prokop and R.S. Sharp, *Performance enhancement of limited bandwidth active automotive suspensions by road preview*, IEE Proc. Control Theory and Applications 142(2) (1995), pp. 140–148.
[26] R.S. Sharp and V. Valtetsiotis, *Optimal preview car steering control*, P. Lugner and K. Hedrick, eds., Supplement to Vehicle System Dynamics Vol. 35 Swets and Zeitlinger, Lisse, 2001, pp. 101–117.
[27] R.S. Sharp, *Driver steering control and a new perspective on car handling qualities*, Journal of Mechanical Engineering Science 219(C8) (2005), pp. 1041–1051.
[28] R.S. Sharp, *Optimal linear time-invariant preview steering control for motorcycles*, S. Bruni and G.R.M. Mastinu, eds., Supplement to Vehicle System Dynamics, Vol. 44 Taylor and Francis, London, 2006, pp. 329–340.
[29] R.S. Sharp, *Optimal preview speed-tracking control for motorcycles*, Multibody System Dynamics 18(3) (2007), pp. 397–411.
[30] R.S. Sharp, *Motorcycle steering control by road preview*, Transactions of ASME, Journal of Dynamic Systems, Measurement and Control 129(4) (2007), pp. 373–381.
[31] R.S. Sharp, *Optimal stabilisation and path-following controls for a bicycle*, Journal of Mechanical Engineering Science 221(4) (2007), pp. 415–428.
[32] R.S. Sharp, *Application of optimal preview control to speed tracking of road vehicles*, Journal of Mechanical Engineering Science 221(12) (2007), pp. 1571–1578.
[33] M. Thommyppillai, S. Evangelou, and R.S. Sharp, *Development of a high-performance virtual car driver for application to motor-racing*, Multibody System Dynamics (2008), in review.
[34] G. Prokop, *Modelling human vehicle driving by model predictive on-line optimisation*, Vehicle System Dynamics 35(1) (2001), pp. 19–35.
[35] R. Frezza and D. Minen, *A new model based driver program for virtual cars in closed loop simulation*, in *The Dynamics of Vehicles on Roads and on Railway Tracks*, Aug, , Milan, Italy, 2005.
[36] J. Edelmann et al., *A passenger car driver model for higher lateral accelerations*, Vehicle System Dynamics 45(12) (2007), pp. 1117–1129.
[37] J.C. Dixon *Tires, Suspension and Handling*, 2nd SAE, Warrendale, 1996.
[38] H.B. Pacejka *Tyre and Vehicle Dynamics*, Butterworth Heinemann, Oxford, 2002 ISBN 0-7506-5141-5.
[39] B.D.O. Anderson and J.B. Moore *Optimal Control: Linear Quadratic Methods*, Prentice Hall, Englewood Cliffs, NJ, 1989.
[40] N. Louam, D.A. Wilson, and R.S. Sharp, *Optimisation and performance enhancement of limited bandwidth active suspensions for automobiles under preview of the road*, Vehicle System Dynamics 21(1) (1992), pp. 39–63.
[41] A. Hazell, *Discrete-time optimal preview control*, Imperial College London Doctoral Thesis, 2008.
[42] R.S. Sharp and D. Pan, *On active roll control for automobiles*, in *Proc. 12^{th} IAVSD Symposium on The Dynamics of Vehicles on Roads and on Railway Tracks*G. Sauvage ed., Swets and Zeitlinger, Lisse, Lyon, 1992, pp. 566–583.